



Smoothing propeller tip geometry for use in a RANS solver

David Hally

Defence R&D Canada – Atlantic

Technical Memorandum
DRDC Atlantic TM 2013-178
October 2013

This page intentionally left blank.

Smoothing propeller tip geometry for use in a RANS solver

David Hally

Defence Research and Development Canada – Atlantic

Technical Memorandum

DRDC Atlantic TM 2013-178

October 2013

© Her Majesty the Queen in Right of Canada (Department of National Defence), 2013

© Sa Majesté la Reine en droit du Canada (Ministère de la Défense nationale), 2013

Abstract

The traditional method of specifying propeller geometry is to define a series of airfoil sections each of which is modified by local values of the chord length, pitch, skew angle and rake. Near the tip of the propeller, where the chord length reduces rapidly to zero, a blade defined in this way often has surface irregularities which make meshing for flow solvers difficult. Methods are described for smoothing the irregularities and saving the resulting propeller geometry in the IGES format which can be read by most flow solvers.

Résumé

La méthode classique pour établir de manière détaillée la géométrie d'une hélice consiste à définir une série de sections de surface portante, chacune d'entre elles étant modifiée en fonction des valeurs localisées de la longueur de corde, du pas de l'hélice, de l'angle oblique et de l'angle d'inclinaison. Près des extrémités de l'hélice, où la longueur de corde diminue rapidement et atteint zéro, la pale définie à l'aide de ces éléments présente souvent une surface irrégulière, ce qui rend complexe le maillage dans le cas des solveurs d'écoulement. Le présent document contient la description de méthodes permettant de lisser les irrégularités de la surface et de sauvegarder les résultats obtenus en matière de géométrie de l'hélice en format IGES, lequel peut être lu par la plupart des solveurs d'écoulement.

This page intentionally left blank.

Executive summary

Smoothing propeller tip geometry for use in a RANS solver

David Hally; DRDC Atlantic TM 2013-178; Defence Research and Development Canada – Atlantic; October 2013.

Background: The design of propellers affects ship performance in many ways including maximum speed, fuel consumption, wear on shafts and machinery, on-board vibrations and radiated noise. The evaluation of propeller designs will be an important part of the projects to acquire the Arctic/Offshore Patrol Ship (AOPS), the Joint Support Ship (JSS) and other vessels for the Royal Canadian Navy.

The use of Reynolds-averaged Navier-Stokes (RANS) flow solvers for evaluating propellers is becoming increasingly common as they have the potential to be more accurate than older panel-based methods. However, before they can be used, an accurate propeller geometry must be available so that an appropriate computational mesh can be created around the propeller.

Principal results: This report describes a method for avoiding problems in the propeller geometry near the tip which can arise when traditional methods of describing a propeller are used. The resulting geometry is smooth, has no coordinate singularities, and has surfaces with edges that match to very high accuracy, all properties that are required when creating grids for flow solvers. Tight control is maintained over the amount by which the smoothed surface can deviate from the original, ensuring that the new geometry remains an accurate representation of the real propeller.

Significance of results: Use of the algorithms described in the report will allow analyses of propellers to be performed with a minimum of effort. The analysis procedure will be more robust and the results more reliable. It is expected that the new method will be used to support the acquisition of propellers for AOPS, JSS and other vessels for the Royal Canadian Navy.

Sommaire

Smoothing propeller tip geometry for use in a RANS solver

David Hally ; DRDC Atlantic TM 2013-178 ; Recherche et développement pour la défense Canada – Atlantique ; octobre 2013.

Introduction : La conception des hélices a de nombreux effets sur le rendement d'un navire, y compris sur des facteurs comme la vitesse maximale, la consommation de combustible, l'usure des arbres et des machines, et l'ampleur des vibrations produites à bord du navire et du bruit rayonné. L'évaluation des modèles d'hélice constituera un élément important des projets d'acquisition de navires de patrouille extracôtiers de l'Arctique (NPEA), de navires de soutien interarmées (NSI) et d'autres bâtiments de la Marine royale canadienne.

L'utilisation de solveurs d'écoulement basés sur l'analyse d'équations de Navier Stokes avec moyennisation des nombres de Reynolds (RANS) est de plus en plus courante dans le cadre d'évaluations d'hélices, car ils pourraient offrir des résultats plus exacts que les anciennes méthodes basées sur la modélisation de panneaux. Avant de pouvoir employer efficacement de tels solveurs, il faut toutefois pouvoir établir de manière exacte la géométrie de l'hélice afin de pouvoir garantir la justesse du maillage numérique créé autour de l'hélice.

Résultats : Le présent rapport comprend la description d'une méthode qui permet d'éviter les problèmes associés à la géométrie de l'hélice près de ses extrémités, qui peuvent se présenter lorsque des méthodes classiques sont employées. La géométrie de l'hélice résultante est lisse et ne comporte pas de singularité en matière de coordonnées, et de plus, les bords de ses surfaces s'ajustent avec une très grande exactitude. Les propriétés de ce type sont toutes cruciales lors de la création de grilles pour un solveur d'écoulement. La méthode assure aussi une régulation serrée de la variation de la surface lissée par rapport à celle d'origine, ce qui permet de garantir que la nouvelle géométrie de l'hélice représente avec exactitude celle de l'hélice réelle.

Portée : L'utilisation des algorithmes décrits dans le présent rapport permettra d'effectuer, avec un minimum d'efforts, l'analyse d'hélices. La technique d'analyse sera plus robuste et les résultats plus fiables. On prévoit que la nouvelle méthode facilitera le processus d'acquisition, par la Marine royale canadienne, d'hélices de NPEA, de NSI et d'autres bâtiments.

Table of contents

Abstract	i
Résumé	i
Executive summary	iii
Sommaire	iv
Table of contents	v
List of figures	vi
1 Introduction	1
2 Coordinate systems	1
3 Overview of blade smoothing	3
4 Defining the blade surfaces	4
5 Calculating the edges of the central surfaces	7
6 Calculating a blade cut	8
7 Smoothing a blade cut	11
8 Calculating the curves around the leading and trailing edges	12
9 Making spline representations of the surfaces	16
10 Defining the hub surface	17
11 Saving the geometry in an IGES file	20
12 Concluding remarks	20
References	22
List of symbols	23

List of figures

Figure 1:	The Cartesian coordinate system.	2
Figure 2:	The five surfaces on the reference blade.	3
Figure 3:	The series of curves on the blade surface passing around the leading and trailing edges.	4
Figure 4:	The points used to split the blade into separate surfaces.	5
Figure 5:	The curves used to split the blade into separate surfaces.	7
Figure 6:	The cubic B-spline function with knots $\{-1, -\frac{1}{2}, 0, \frac{1}{2}, 1\}$ used to modulate the smoothing.	12
Figure 7:	The curve \mathbf{c}_{LETE}	12
Figure 8:	The effect of the location of s_j (shown by the red dots) on the leading and trailing edge curves of a highly skewed blade. When s_j is close to the tip (left) the curves can show excessive curvature; lowering s_j (right) makes a significant improvement. . .	16
Figure 9:	The full propeller (left) and the portion saved in the IGES file (right).	18
Figure 10:	The curves delimiting the hub sector in the hub parameter space.	19

1 Introduction

Traditionally the geometry of a propeller blade is defined by specifying a series of airfoil sections from the root of the blade to its tip. Each section is modified by the local values of the chord length, pitch, skew angle and rake. The resulting curves can be interpolated to provide a full geometric description of the blade. Software has been developed at DRDC Atlantic for reading section data for a blade and generating a geometric representation that can be used in a variety of applications [1].

Two problems arise when the propeller geometry generated in this way is used in Computational Fluid Dynamics (CFD) programs for calculating the flow around the propeller:

1. Commercial CFD programs do not use the DRDC Atlantic representation of the propeller; it must be converted to a form that they can use.
2. The modulation of the blade sections by the chord length, rake, etc. can result in very rapidly varying geometry near the blade tip where there is a coordinate singularity. The geometry in this region must be smoothed to prevent problems with generating meshes for the CFD calculations, and with the results of the calculations themselves (e.g. spurious pressure peaks caused by flow over geometric corners that would be smoother on a real propeller).

The methods described in this report address both these problems. It describes algorithms for modifying the propeller geometry to avoid the coordinate singularity at the tip and to smooth it in a controlled way. The algorithms have been implemented in the program `smooth-prop` [2]; it saves the smoothed propellers in IGES format [3] which can be read by most commercial CFD programs.

2 Coordinate systems

The propeller is defined using a Cartesian coordinate system attached to the propeller in which the origin is the point at which the propeller reference line meets the propeller axis. The z coordinate increases from upstream to downstream along the propeller axis. The y coordinate increases outward from the propeller axis along the propeller reference line. The x coordinate is perpendicular to y and z such that the coordinate system is right-handed; it increases to starboard when the tip of the reference blade is at top dead centre. The Cartesian coordinate system is illustrated in Fig. 1.

The reference propeller blade is parameterized using ξ and η ; a point on the blade will be denoted by $\mathbf{b}(\xi, \eta)$. On all blades η increases from 0.0 at the propeller axis to 1.0 at the blade tip. Typically there is a minimum value of η below which the

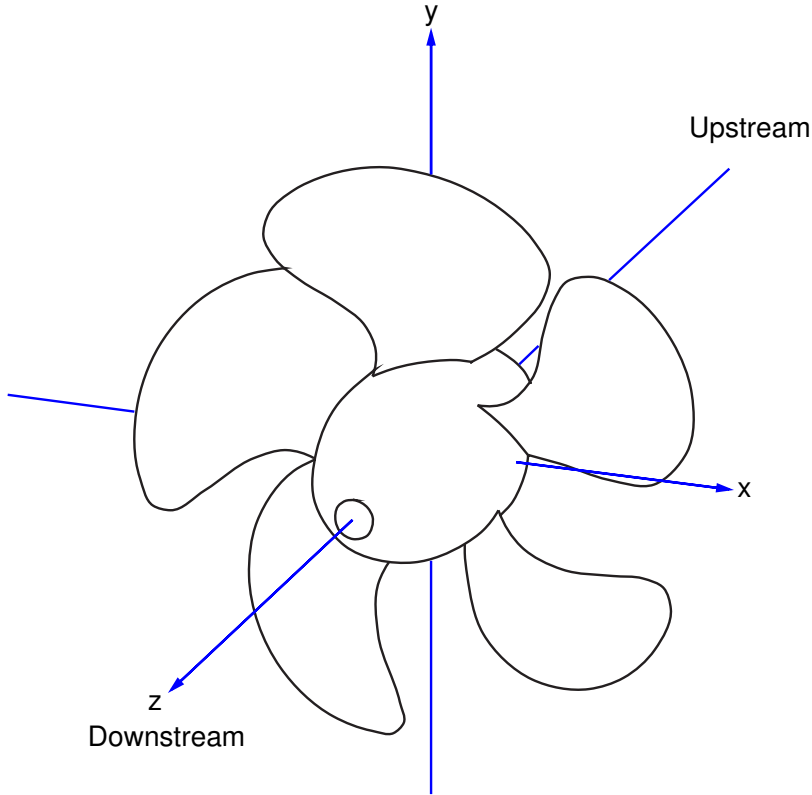


Figure 1: *The Cartesian coordinate system.*

reference blade geometry is undefined. For convenience, the two-vector in the blade parameter space, (ξ, η) , will sometimes be denoted \mathbf{p} .

On a right-handed blade, ξ increases along the pressure side of the blade from 0.0 at the trailing edge to 0.5 at the leading edge, then increases along the suction side of the blade to 1.0 at the trailing edge. On a left-handed blade ξ increases first along the suction side, then along the pressure side. This ensures that a normal to the blade defined by

$$\mathbf{n} = \frac{\partial \mathbf{b}}{\partial \xi} \times \frac{\partial \mathbf{b}}{\partial \eta} \quad (1)$$

is always outward pointing.

The algorithms described in this report assume that the trailing edge of the blade is closed ($\mathbf{b}(0, \eta) = \mathbf{b}(1, \eta)$) and blunt (the unit normal at $(0, \eta)$ is equal to the unit normal at $(1, \eta)$). The DRDC propeller geometry classes include methods for ensuring that the trailing edge is closed and blunt: see [Ref. 1](#), Secs. 6.2.2 and 6.2.6.

By defining $\mathbf{b}(\xi - 1, \eta) = \mathbf{b}(\xi, \eta)$, the blade parameterization can be made periodic in ξ . Since the trailing edge is closed and blunt, the resulting periodic version of the blade is continuous and smooth across the trailing edge.

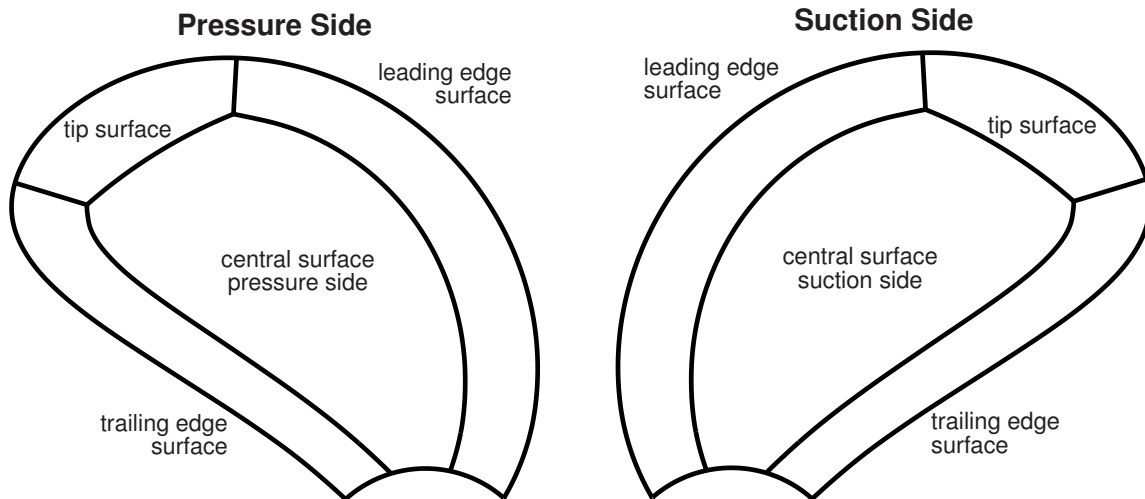


Figure 2: *The five surfaces on the reference blade.*

3 Overview of blade smoothing

The blade tip smoothing and subsequent saving of the hull in IGES format is done using the following steps.

1. A file is read which specifies the propeller geometry in the DRDC format (see [Ref. 1, Sec. 9.4](#)).
2. The reference blade surface is split into five separate surfaces as shown in [Fig. 2](#). The tip, leading edge and trailing edge surfaces each wrap around the leading/trailing edge from the pressure side to the suction side.
3. A series of curves is calculated, each curve lying on one of the blade surfaces passing around the leading and trailing edges. An example of the curves is shown in [Fig. 3](#).
4. Each curve is sampled to obtain a series of points to which a weighted Laplace filter is applied to smooth the points near the leading and trailing edges.
5. The smoothed points are splined to generate a new sequence of curves.
6. The series of curves is then splined to generate new blade surfaces.
7. Curves are defined which mark the limits of the hub sector associated with the reference blade with the blade footprint removed.
8. The splined blade surfaces and the trimmed hub surface are written to an output file in IGES format.

Details of each step in the procedure are explained in the sections which follow.

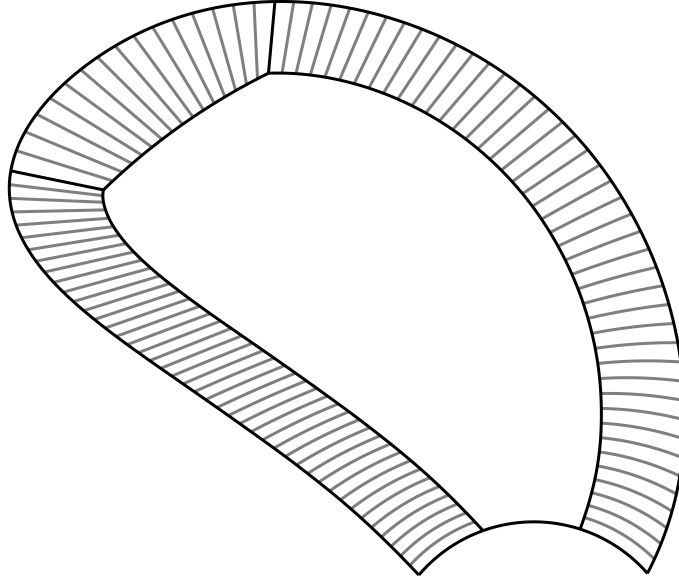


Figure 3: The series of curves on the blade surface passing around the leading and trailing edges.

4 Defining the blade surfaces

The five surfaces into which the blade is split are defined using six points:

1. $\mathbf{x}_{LL} = \mathbf{b}(\mathbf{p}_{LL})$, a point on the blade-hub intersection at the lower left hand corner of the central surface on the pressure side of the blade. This point is specified using the value of ξ alone; the value of η is determined by the constraint that the point lies on the hub. The DRDC propeller geometry classes provide a curve, $\eta_h(\xi)$, such that $\mathbf{b}(\xi, \eta_h(\xi))$ lies on the hub: see Ref. 1, Sec. 9.1.6. Therefore $\mathbf{p}_{LL} = (\xi_{LL}, \eta_h(\xi_{LL}))$.
2. $\mathbf{x}_{LR} = \mathbf{b}(\mathbf{p}_{LR})$ with $\mathbf{p}_{LR} = (\xi_{LR}, \eta_h(\xi_{LR}))$. This is a point on the blade-hub intersection at the lower right hand corner of the central surface on the pressure side of the blade.
3. $\mathbf{x}_{UL} = \mathbf{b}(\mathbf{p}_{UL})$, a point at the upper left hand corner of the central surface on the pressure side of the blade.
4. $\mathbf{x}_{UR} = \mathbf{b}(\mathbf{p}_{UR})$, a point on the blade hub intersection at the upper right hand corner of the central surface on the pressure side of the blade.
5. $\mathbf{x}_{LE} = \mathbf{b}(\mathbf{p}_{LE})$ with $\mathbf{p}_{LE} = (\frac{1}{2}, \eta_{LE})$. This is a point on the leading edge.
6. $\mathbf{x}_{TE} = \mathbf{b}(\mathbf{p}_{TE})$ with $\mathbf{p}_{TE} = \mathbf{b}(0, \eta_{TE})$. This is a point on the trailing edge.

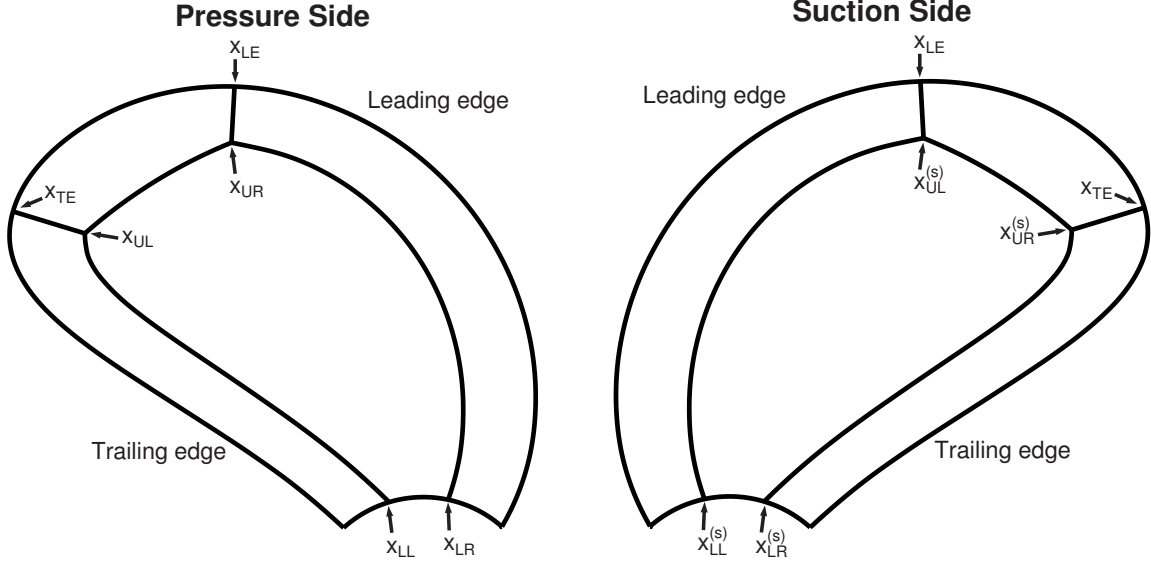


Figure 4: The points used to split the blade into separate surfaces.

Each of the corner points of the central surface has a corresponding point on the suction side of the blade obtained by changing its ξ value to $1 - \xi$: i.e. $\mathbf{x}_{LR}^{(s)} = \mathbf{b}(1 - \xi_{LL}, \eta_h(1 - \xi_{LL}))$, $\mathbf{x}_{LL}^{(s)} = \mathbf{b}(1 - \xi_{LR}, \eta_h(1 - \xi_{LR}))$, $\mathbf{x}_{UR}^{(s)} = \mathbf{b}(1 - \xi_{UL}, \eta_{UL})$, $\mathbf{x}_{UL}^{(s)} = \mathbf{b}(1 - \xi_{UR}, \eta_{UR})$, where the superscript (s) denotes the suction side of the blade.

The ten points are shown in Fig. 4.

These points are used to define twelve edge curves, each using a single parameter, u , in the range $[0, 1]$:

1. $\mathbf{c}_1(u)$: the curve along the blade-hub intersection wrapping around the trailing edge between points $\mathbf{x}_{LR}^{(s)}$ and \mathbf{x}_{LL} :

$$\mathbf{c}_1(u) = \mathbf{b}\left(\xi(u), \eta_h(\xi(u))\right); \quad \xi(u) = (2u - 1)\xi_{LL}. \quad (2)$$

2. $\mathbf{c}_2(u)$: the curve along the blade-hub intersection between points \mathbf{x}_{LL} and \mathbf{x}_{LR} :

$$\mathbf{c}_2(u) = \mathbf{b}\left(\xi(u), \eta_h(\xi(u))\right); \quad \xi(u) = \xi_{LL} + u(\xi_{LR} - \xi_{LL}). \quad (3)$$

3. $\mathbf{c}_3(u)$: the curve along the blade-hub intersection wrapping around the leading edge between points \mathbf{x}_{LR} and $\mathbf{x}_{LL}^{(s)}$:

$$\mathbf{c}_3(u) = \mathbf{b}\left(\xi(u), \eta_h(\xi(u))\right); \quad \xi(u) = \xi_{LR} + u(\xi_{LL}^{(s)} - \xi_{LR}). \quad (4)$$

4. $\mathbf{c}_4(u)$: the curve along the blade-hub intersection between points $\mathbf{x}_{LL}^{(s)}$ and $\mathbf{x}_{LR}^{(s)}$:

$$\mathbf{c}_3(u) = \mathbf{b}\left(\xi(u), \eta_h(\xi(u))\right); \quad \xi(u) = \xi_{LL}^{(s)} + u(\xi_{LR}^{(s)} - \xi_{LL}^{(s)}). \quad (5)$$

5. $\mathbf{c}_5(u)$: the curve on the left edge of the central surface on the pressure side. It runs between points \mathbf{x}_{LL} and \mathbf{x}_{UL} . The method of calculating this curve is described in [Sec. 5](#).
6. $\mathbf{c}_6(u)$: the curve on the right edge of the central surface on the pressure side. It runs between points \mathbf{x}_{LR} and \mathbf{x}_{UR} . The method of calculating this curve is described in [Sec. 5](#).
7. $\mathbf{c}_7(u)$: the curve on the left edge of the central surface on the suction side. It runs between points $\mathbf{x}_{LL}^{(s)}$ and $\mathbf{x}_{UL}^{(s)}$. The method of calculating this curve is described in [Sec. 5](#).
8. $\mathbf{c}_8(u)$: the curve on the right edge of the central surface on the suction side. It runs between points $\mathbf{x}_{LR}^{(s)}$ and $\mathbf{x}_{UR}^{(s)}$. The method of calculating this curve is described in [Sec. 5](#).
9. $\mathbf{c}_9(u)$: the curve at the top of the central surface on the pressure side. It runs between points \mathbf{x}_{UL} and \mathbf{x}_{UR} :

$$\mathbf{c}_9(u) = \mathbf{b}\left(\mathbf{p}(u)\right); \quad \mathbf{p}(u) = \mathbf{p}_{UL} + u(\mathbf{p}_{UR} - \mathbf{p}_{UL}). \quad (6)$$

10. $\mathbf{c}_{10}(u)$: the curve at the top of the central surface on the suction side. It runs between points $\mathbf{x}_{UL}^{(s)}$ and $\mathbf{x}_{UR}^{(s)}$:

$$\mathbf{c}_{10}(u) = \mathbf{b}\left(\mathbf{p}(u)\right); \quad \mathbf{p}(u) = \mathbf{p}_{UL}^{(s)} + u(\mathbf{p}_{UR}^{(s)} - \mathbf{p}_{UL}^{(s)}). \quad (7)$$

11. $\mathbf{c}_{11}(u)$: the curve at the top of the surface wrapping around the trailing edge. It is the intersection of the blade with the plane containing the points \mathbf{x}_{UL} , \mathbf{x}_{TE} and $\mathbf{x}_{UR}^{(s)}$. The method of calculating this curve is described in [Sec. 6](#).
12. $\mathbf{c}_{12}(u)$: the curve at the top of the surface wrapping around the leading edge. It is the intersection of the blade with the plane containing the points \mathbf{x}_{UR} , \mathbf{x}_{LE} and $\mathbf{x}_{UL}^{(s)}$. The method of calculating this curve is described in [Sec. 6](#).

The twelve curves are shown in [Fig. 5](#).

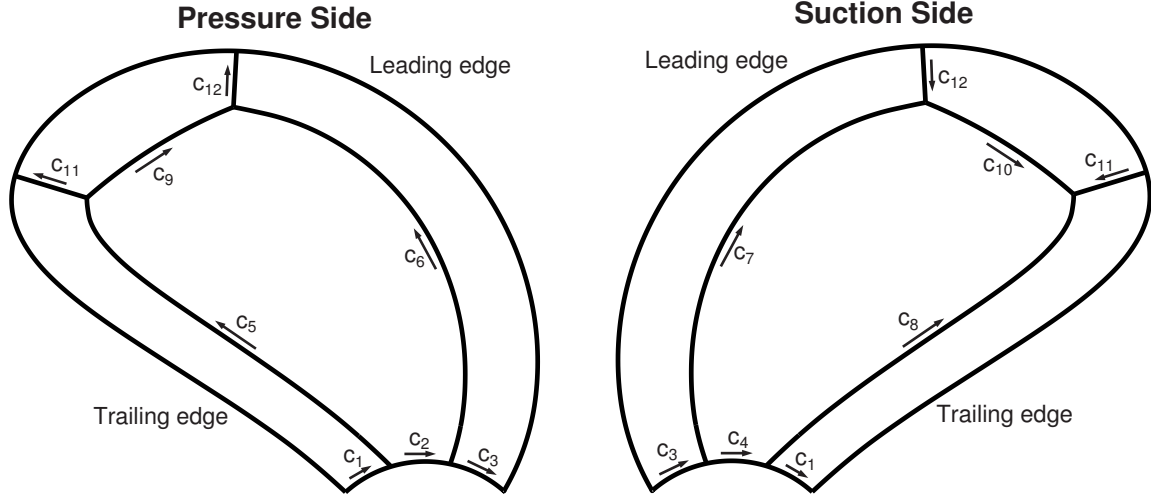


Figure 5: The curves used to split the blade into separate surfaces.

5 Calculating the edges of the central surfaces

The curves along the sides of the central domains, $\mathbf{c}_5(u)$, $\mathbf{c}_6(u)$, $\mathbf{c}_7(u)$ and $\mathbf{c}_8(u)$, are calculated such that the distance of the curve from the leading or trailing edge varies roughly linearly along the length of the curve. Therefore, if the two end-points are the same distance from the leading edge, the whole curve is equidistant from the leading edge and the surface wrapping around the leading edge has a nearly constant width. When a computational grid is created on the surface [4], this makes it easy to maintain a nearly constant size for the computational cells near the leading edge. This comes at the expense of more irregularity of the cells in the central domains, but that is typically not a critical region of the flow, so greater irregularity can be tolerated there.

To calculate the curve along the right side of the central surface on the pressure side, $\mathbf{c}_6(u)$, two subsidiary curves are calculated. The first is a straight line in blade parameter space between \mathbf{p}_{LR} and \mathbf{p}_{UR} :

$$\mathbf{p}_1(u) = \mathbf{p}_{LR} + a_1(u)(\mathbf{p}_{UR} - \mathbf{p}_{LR}) \quad (8)$$

where $a_1(u)$ is an arclength distribution (see Ref. 5, Sec. 15) whose purpose is to convert the parameterization to the fractional arclength along the curve.

The second runs along the leading edge between the point where the leading edge meets the hub, $\mathbf{p}_h = \left(\frac{1}{2}, \eta_h\left(\frac{1}{2}\right)\right)$, and \mathbf{p}_{LE} :

$$\mathbf{p}_2(u) = \mathbf{p}_h + a_2(u)(\mathbf{p}_{LE} - \mathbf{p}_h) \quad (9)$$

where $a_2(u)$ is also an arclength distribution converting the parameterization to fractional arclength.

Let d_{LR} be the distance of \mathbf{x}_{LR} from the point where the leading edge meets the hub and let d_{UR} be the distance of \mathbf{x}_{UR} from \mathbf{x}_{LE} :

$$d_{LR} = \left| \mathbf{b}(\mathbf{p}_1(0)) - \mathbf{b}(\mathbf{p}_2(0)) \right|; \quad d_{UR} = \left| \mathbf{b}(\mathbf{p}_1(1)) - \mathbf{b}(\mathbf{p}_2(1)) \right|. \quad (10)$$

Define the distance function

$$d(u) = d_{LR} + u(d_{UR} - d_{LR}). \quad (11)$$

For a given u , we find the point on the straight line joining $\mathbf{b}(\mathbf{p}_1(u))$ and $\mathbf{b}(\mathbf{p}_2(u))$ that is a distance $d(u)$ from the leading edge:

$$\mathbf{x}_m(u) = \mathbf{b}(\mathbf{p}_2(u)) + \frac{d(u) \left(\mathbf{b}(\mathbf{p}_1(u)) - \mathbf{b}(\mathbf{p}_2(u)) \right)}{\left| \mathbf{b}(\mathbf{p}_1(u)) - \mathbf{b}(\mathbf{p}_2(u)) \right|}. \quad (12)$$

Notice that $\mathbf{x}_m(0) = \mathbf{b}(\mathbf{p}_1(0)) = \mathbf{x}_{LR}$ and $\mathbf{x}_m(1) = \mathbf{b}(\mathbf{p}_1(1)) = \mathbf{x}_{UR}$. At other values of u , $\mathbf{x}_m(u)$ is an approximation of $\mathbf{c}_6(u)$ but it does not lie on the blade surface. To project it onto the blade, let the unit normal to the blade at $\mathbf{p}_1(u)$ be \hat{n} and construct a line parallel to \hat{n} through $\mathbf{x}_m(u)$. Find the point where this line meets the blade on the pressure side by solving the three components of

$$\mathbf{b}(\mathbf{p}_m) = \mathbf{x}_m(u) + t\hat{n} \quad (13)$$

for the three unknowns t and the two components of \mathbf{p}_m . This is done using the Newton-Raphson method for N values of u yielding a sequence of parameters \mathbf{p}_i for $i \in [1, N]$. A cubic spline is passed through the parameters to generate the curve $\mathbf{p}(u)$. The curve $\mathbf{c}_6(u)$ is then defined by the spline composed with the blade surface:

$$\mathbf{c}_6(u) = \mathbf{b}(\mathbf{p}(u)). \quad (14)$$

The three curves $\mathbf{c}_5(u)$, $\mathbf{c}_7(u)$ and $\mathbf{c}_8(u)$ are defined using a similar method.

6 Calculating a blade cut

A blade cut through the leading edge is defined as the intersection of the blade with a plane passing through three points, $\mathbf{x}_0 = \mathbf{b}(\xi, \eta)$, $\mathbf{x}_1 = \mathbf{b}(\frac{1}{2}, \eta_e)$ and $\mathbf{x}_2 = \mathbf{b}(1 - \xi, \eta)$ with $\xi < \frac{1}{2}$. The point \mathbf{x}_0 is on the pressure side, \mathbf{x}_1 is on the leading edge, and \mathbf{x}_2 is on the suction side. A normal to the plane is

$$\mathbf{n} = (\mathbf{x}_1 - \mathbf{x}_0) \times (\mathbf{x}_1 - \mathbf{x}_2); \quad \hat{n} = \frac{\mathbf{n}}{|\mathbf{n}|}. \quad (15)$$

Consider a point on the blade having blade parameters ξ and η . If it lies on the cut, then it also lies in the plane, so that

$$\left(\mathbf{b}(\xi, \eta) - \mathbf{x}_0\right) \cdot \hat{\mathbf{n}} = 0. \quad (16)$$

Suppose that $\mathbf{b}(\xi_i, \eta_i)$ lies on the cut. Let $(\xi_{i+1}, \eta_{i+1}) = (\xi_i + \Delta\xi, \eta_i + \Delta\eta)$ and suppose that $\mathbf{b}(\xi_{i+1}, \eta_{i+1})$ also lies on the cut. Then

$$\begin{aligned} 0 &= \left(\mathbf{b}(\xi_{i+1}, \eta_{i+1}) - \mathbf{x}_0\right) \cdot \hat{\mathbf{n}} \\ &\approx \left(\mathbf{b}(\xi_i, \eta_i) - \mathbf{x}_0\right) \cdot \hat{\mathbf{n}} + \left(\Delta\xi \mathbf{b}_\xi(\xi_i, \eta_i) + \Delta\eta \mathbf{b}_\eta(\xi_i, \eta_i)\right) \cdot \hat{\mathbf{n}} \\ &= \left(\Delta\xi \mathbf{b}_\xi(\xi_i, \eta_i) + \Delta\eta \mathbf{b}_\eta(\xi_i, \eta_i)\right) \cdot \hat{\mathbf{n}} \end{aligned} \quad (17)$$

where \mathbf{b}_ξ and \mathbf{b}_η denote the partial derivatives of \mathbf{b} with respect to ξ and η respectively. Therefore, in the (ξ, η) parameter space, a tangent to the cut is:

$$\mathbf{t} = \left(-\mathbf{b}_\eta(\xi_i, \eta_i) \cdot \hat{\mathbf{n}}, \mathbf{b}_\xi(\xi_i, \eta_i) \cdot \hat{\mathbf{n}}\right); \quad \hat{t} = \frac{\mathbf{t}}{|\mathbf{t}|} \quad (18)$$

and

$$(\Delta\xi, \Delta\eta) = \alpha \hat{\mathbf{t}} \quad (19)$$

where α is the distance between the points in the parameter space.

The values of $\Delta\xi$ and $\Delta\eta$ can be used as a first guess for a new point on the cut a distance of approximately α from the previous point. Then the line in parameter space defined by

$$\xi(s) = \xi_{i+1} + s\Delta\eta; \quad \eta(s) = \eta_{i+1} - s\Delta\xi \quad (20)$$

is perpendicular to the line joining (ξ_i, η_i) and $(\xi_i + \Delta\xi, \eta_i + \Delta\eta)$. To refine the guess, search for the point lying on the intersection of this line and the cut: i.e. the point satisfying Eqs. (16) and (20). A Newton-Raphson search is used to find the independent variable s .

The Newton-Raphson search will converge quickly for most points but near the tip, where the angle between the ξ and η coordinate lines becomes very small, it may fail. In that case a search in which ξ is the parameter is tried: i.e. a Newton-Raphson search is used to solve

$$\left[\mathbf{b}(\xi, \eta_i + \Delta\eta) - \mathbf{x}_0\right] \cdot \hat{\mathbf{n}} = 0. \quad (21)$$

for ξ . If the second attempt fails, a third attempt is made using a simple bisection search for s :

1. Find two values of s given points lying on either side of the cut plane: i.e. find s_1 and s_2 such that

$$\left[\mathbf{b}(\xi(s_1), \eta(s_1)) - \mathbf{x}_0\right] \cdot \hat{\mathbf{n}} < 0; \quad \left[\mathbf{b}(\xi(s_2), \eta(s_2)) - \mathbf{x}_0\right] \cdot \hat{\mathbf{n}} > 0. \quad (22)$$

2. Let $s_3 = \frac{1}{2}(s_1 + s_2)$.
3. If $\left[\mathbf{b}(\xi(s_3), \eta(s_3)) - \mathbf{x}_0 \right] \cdot \hat{n} < 0$, set s_1 to s_3 ; otherwise set s_2 to s_3 .
4. Repeat until $\left| \mathbf{b}(\xi(s_1), \eta(s_1)) - \mathbf{b}(\xi(s_2), \eta(s_2)) \right|$ is sufficiently small.

The process can now be repeated to find another point, (ξ_{i+2}, η_{i+2}) , further along the cut. A collection of points along the length of the cut can then be obtained.

Since the curvature of the blade is very high at the leading and trailing edges and quite small elsewhere, the distance between the points, α , is adjusted as the point \mathbf{x}_1 is approached.

$$\alpha = 0.003 \left(1 - \frac{0.999 |\mathbf{b}(\xi, \eta) - \mathbf{x}_0|}{|\mathbf{x}_1 - \mathbf{x}_0|} \right) \quad (23)$$

giving α a maximum value of 3×10^{-3} and a minimum value of 3×10^{-6} . Since α is a distance in parameter space and changing ξ or η by 1.0 causes a change in real space of about one blade radius, R , the distance between the points in real space ranges from roughly $3 \times 10^{-6}R$ to $3 \times 10^{-3}R$.

Let $\{ \mathbf{p}_i = (\xi_i, \eta_i) : i \in [1, N] \}$ denote the sequence of points in the blade parameter space. Let m be the value of i for which the point lies on the leading or trailing edge. A spline through the points is calculated as follows to yield a parameter curve.

1. The arclength in parameter space at each point is calculated:
 $a_1 = 0$; $a_i = a_{i-1} + |\mathbf{p}_i - \mathbf{p}_{i-1}|$ for $i > 1$.
2. A sequence of spline knots, t_i , is calculated using

$$t_i = \frac{a_i}{a_N} \left[1 + \frac{(a_N - a_i)(a_N - 2a_m)}{2a_m(a_N - a_m)} \right]. \quad (24)$$

Note that $t_1 = 0$, $t_m = \frac{1}{2}$ and $t_N = 1$.

3. A cubic spline is calculated through the sequences (t_i, ξ_i) and (t_i, η_i) to yield the parameter curve. Eq. (24) ensures that when the spline is evaluated at $t = \frac{1}{2}$, the point returned is on the leading or trailing edge.

Notice that, because the spline is generated in parameter space, the generated blade cut still lies exactly on the blade despite any errors due to the spline interpolation or inaccuracies in the Newton-Raphson search for the points on the cut.

A blade cut through the trailing edge is calculated in a similar way using the periodic version of the blade to ensure that the blade cut is continuous in parameter space as it crosses the trailing edge.

7 Smoothing a blade cut

A blade cut is smoothed by first sampling to generate a series of points along the cut, then applying a smoothing filter to the points, then regenerating the curve by passing a spline through the smoothed points. The sampled points are independent of the points used to generate the parameter curve of the cut. This allows the number of points to be different and their spacing to be controlled so that the smoothing algorithm will operate effectively.

Let d be the maximum separation of the sampled points, h their separation at the leading or trailing edge, and let $\mathbf{p}(s)$ be the splined parameter curve defining the cut as defined in the previous section. Then the points are $\mathbf{y}_i = \mathbf{b}(\mathbf{p}(s_i))$ with

$$s_i = f\left(\frac{i-1}{N-1}\right); \quad f(x) = \begin{cases} \frac{1}{2}g(2x) & \text{for } 0 \leq x \leq \frac{1}{2}; \\ \frac{1}{2} + \frac{1}{2}g(2x-1) & \text{for } \frac{1}{2} \leq x \leq 1; \end{cases} \quad (25)$$

$$g(x) = \frac{h(x)}{\alpha + (1-\alpha)h(x)}; \quad h(x) = \frac{1}{2} \left[1 + \frac{\tanh\left(\left(x - \frac{1}{2}\right)\Delta\right)}{\tanh\left(\frac{1}{2}\Delta\right)} \right]; \quad (26)$$

$$\alpha = \sqrt{\frac{h}{d}}; \quad \frac{\sinh \Delta}{\Delta} = \frac{2L}{(N-1)\sqrt{dh}}; \quad (27)$$

$$r = \frac{L-h}{L-d}; \quad L = |\mathbf{x}_1 - \mathbf{x}_0|; \quad N = 1 + 2 \left\lceil \frac{\ln(d/h)}{\ln(r)} \right\rceil \quad (28)$$

where the curly brackets denote ‘the closest integer to’. The function $g(x)$ is a tanh distribution and the function $f(x)$ represents two tanh distributions spliced together (see Ref. 5, Secs. 11.3 and 13). The choice for the number of points, N , makes the tanh distributions nearly geometric; i.e. the ratio of neighbouring node intervals is nearly constant. Eq. (27) can be solved for Δ using the method described in Ref. 5, Annex A.5. The spacing at the leading and trailing edges, h , is normally set to $d/100$.

Notice that if i is the mid-point (i.e. $i = \frac{1}{2}(N+1)$), then $s_i = \frac{1}{2}$. Therefore, the mid-point lies on the leading or trailing edge, since the blade cut parameter function $\mathbf{p}(s)$ has been constructed so that $\mathbf{p}(\frac{1}{2})$ lies on the leading or trailing edge (see Eq. (24)).

A smoothing filter is applied to the sampled points while leaving the point on the leading or trailing edge unaltered. With $\mathbf{y}_i^{(0)} = \mathbf{y}_i$, the points after n smoothing iterations are:

$$\mathbf{y}_i^n = \mathbf{y}_i^{n-1} + \begin{cases} 0 & \text{if } i = \frac{1}{2}(N+1); \\ \frac{1}{6}\beta_i(-\mathbf{y}_{i-2}^{n-1} + 4\mathbf{y}_{i-1}^{n-1} - 6\mathbf{y}_i^{n-1} + 4\mathbf{y}_{i+1}^{n-1} - \mathbf{y}_{i+2}^{n-1}) & \text{otherwise.} \end{cases} \quad (29)$$

The smoothing factor β_i is adjusted point by point so that the smoothing only occurs within a distance d_e of the leading or trailing edge and within a distance d_t from the

tip. Let a be the arclength along the leading or trailing edge from \mathbf{x}_1 to the tip. Then

$$\beta_i = \alpha f(a/d_t) f(|\mathbf{y}_i - \mathbf{x}_1|/d_e) \quad (30)$$

with α a constant and $f(x)$ a smooth function which is non-zero only in $[-1, 1]$ and for which $f(0) = 1$ is a maximum. It is convenient to set $f(x)$ to the cubic B-spline function with knots $\{-1, -\frac{1}{2}, 0, \frac{1}{2}, 1\}$. It is plotted in Fig. 6.

The sequence of smoothed points, $\{s_i, \mathbf{y}_i\}$, is interpolated using a cubic spline to generate a smoothed version of the blade cut. Note that because the smoothed points do not all lie on the original blade surface, the smoothed blade cut does not have a representation in the parameter space of the blade.

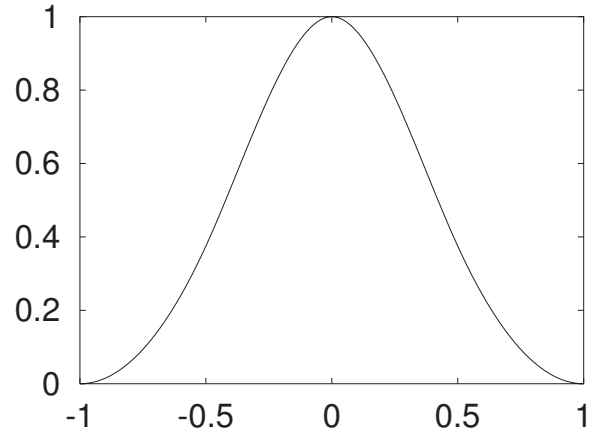


Figure 6: The cubic B-spline function with knots $\{-1, -\frac{1}{2}, 0, \frac{1}{2}, 1\}$ used to modulate the smoothing.

8 Calculating the curves around the leading and trailing edges

In the vicinity of the tip, the curves around the leading and trailing edges are blade cuts: i.e. intersections of planes with the blade. However, this cannot be extended all the way to the hub because the intersection of the blade with the hub does not lie in a plane. On the lower portion of the blade the curves are defined using trans-finite interpolation between a blade cut and the intersection of the blade and hub. The full procedure is as follows.

First a curve, $\mathbf{c}_{LETE}(s)$, is calculated along the trailing edge from the root to the tip, then along the leading edge back to the root. With the help of an arclength distribution (see Ref. 5, Sec. 15), the curve is parameterized using fractional arclength, s , so that $s = 0$ gives the point where the trailing edge meets the hub and $s = 1$ is where the leading edge meets the hub. The total length of this curve is denoted by L .

The representation of $\mathbf{c}_{LETE}(s)$ in blade

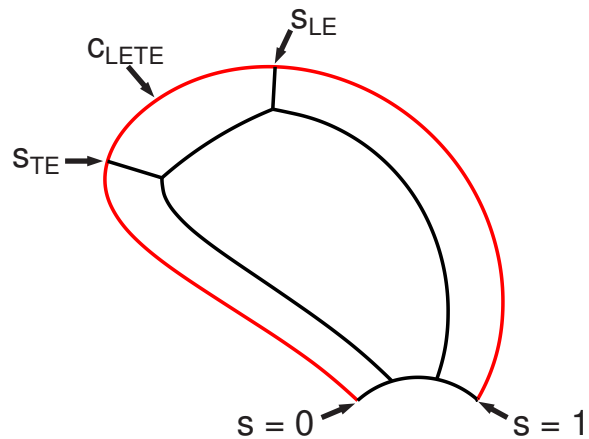


Figure 7: The curve \mathbf{c}_{LETE} .

parameter space will be denoted $\mathbf{p}_{LETE}(s)$: i.e. $\mathbf{b}(\mathbf{p}_{LETE}(s)) = \mathbf{c}_{LETE}(s)$. Note that $\mathbf{p}_{LETE}(s)$ is discontinuous at the tip where the ξ -value jumps from $\frac{1}{2}$ on the leading edge to either 0 or 1 on the trailing edge, but that is inconsequential in the algorithm described below. For the portion along the trailing edge, one could choose the ξ -value of $\mathbf{p}_{LETE}(s)$ to be 0 or 1. Here it is chosen to be 0, which is consistent with the value used on the periodic blade surface used when calculating the blade cuts (see Sec. 6).

The value of s for which $\mathbf{c}_{LETE}(s) = \mathbf{x}_{LE}$ is denoted s_{LE} . Similarly, s_{TE} is defined to satisfy $\mathbf{c}_{LETE}(s_{TE}) = \mathbf{x}_{TE}$ and s_{tip} is the value of s at the blade tip.

The maximum allowed distance between blade cuts as measured along the leading and trailing edge is specified; it is denoted Δc . The number of blade cuts in the upper blade surface, N_t , is then chosen so that their separation is as close to Δc as possible without exceeding it:

$$N_t = \left\lceil \frac{L(s_{LE} - s_{TE})}{\Delta c} \right\rceil + 1. \quad (31)$$

The points defining blade cut $i \in [1, N_t]$ are

$$\mathbf{x}_0 = \mathbf{c}_9(u); \quad \mathbf{x}_1 = \mathbf{c}_{LETE}(s_{TE} + u(s_{LE} - s_{TE})); \quad \mathbf{x}_2 = \mathbf{c}_{10}(1 - u); \quad (32)$$

$$u = \frac{i - 1}{N_t - 1}. \quad (33)$$

As \mathbf{c}_{LETE} is parameterized using fractional arclength, the points \mathbf{x}_1 for successive values of i are equally spaced along \mathbf{c}_{LETE} .

In a similar way a series of blade cuts can be defined on the leading edge surface. We find N_{LE} equally spaced points along curve \mathbf{c}_6 , along \mathbf{c}_{LETE} between s_{LE} and 1, and along curve \mathbf{c}_7 . The points along \mathbf{c}_6 become the points \mathbf{x}_0 for the blade cuts, the points along \mathbf{c}_{LETE} become the points \mathbf{x}_1 , and the points along \mathbf{c}_7 become the points \mathbf{x}_2 . More precisely, let $i \in [1, N_{LE}]$ denote blade cut i . This blade cut is defined using the algorithm described in Sec. 6 using the points

$$\mathbf{x}_0 = \mathbf{c}_6(u); \quad \mathbf{x}_1 = \mathbf{c}_{LETE}(1 - u(1 - s_{LE})); \quad \mathbf{x}_2 = \mathbf{c}_7(u); \quad (34)$$

$$u = \frac{i - 1}{N_{LE} - 1}. \quad (35)$$

If the distance from \mathbf{x}_1 to the tip is less than d_t (i.e. if $(s_{tip} - 1 + u(1 - s_{LE}))L < d_t$), then the blade cut is smoothed.

Note that blade cut N_{LE} is the upper edge of the leading edge surface and blade cut 1 lies near the blade-hub intersection. It would be simple to require that the N_{LE} curves around the leading edge be equal to the N_{LE} blade cuts but, as pointed out above, blade cut 1 cannot be used as the lower edge of the leading edge surface as the blade-hub intersection does not lie in a plane. Instead, one of the blade cuts is chosen

as a transition line; let it be blade cut j . Curve i is equal to blade cut i if $i \geq j$. For $i < j$, curve i is defined using trans-finite interpolation between blade cut j , the blade-hub intersection (curve \mathbf{c}_3), curve \mathbf{c}_6 and curve \mathbf{c}_7 . The interpolation is done in the blade parameter space to ensure that the resulting curves all lie on the blade surface. Let $\mathbf{p}_3(u)$ be the curve in parameter space corresponding to $\mathbf{c}_3(u)$: i.e.

$$\mathbf{b}(\mathbf{p}_3(u)) = \mathbf{c}_3(u). \quad (36)$$

Similarly we can defined parameter curves $\mathbf{p}_6(u)$, $\mathbf{p}_7(u)$ and $\mathbf{p}_c(u)$ corresponding to curves $\mathbf{c}_6(u)$, $\mathbf{c}_7(u)$ and the blade cut j . It is important to note that $\mathbf{p}_c(u)$ will not be defined if blade cut j has been smoothed, since the smoothed cut no longer lies exactly on the blade surface and therefore does not have a representation in the blade parameter space. Therefore blade cut j must be far enough from the tip that it is outside the range of smoothing.

Curve i is now defined by

$$\mathbf{c}_{LEi}(v) = \mathbf{b}(\mathbf{p}(u_i, v)); \quad (37)$$

$$\mathbf{p}(u, v) = \mathbf{q}(\xi(u, v), \eta(u, v)); \quad (38)$$

$$\xi(u, v) = u + 4v(1 - v)(f_u(u) - u); \quad (39)$$

$$\eta(u, v) = v + 4v(1 - v)(f_v(u) - \frac{1}{2}); \quad (40)$$

$$\begin{aligned} \mathbf{q}(u, v) = & \frac{(u_j - u)}{u_j} \mathbf{p}_3(v) + \frac{u}{u_j} \mathbf{p}_c(v) + (1 - v) \mathbf{p}_6(u) + v \mathbf{p}_7(u) \\ & - \frac{(u_j - u)(1 - v)}{u_j} \mathbf{p}_{LL} - \frac{(u_j - u)v}{u_j} \mathbf{p}_{LR}^{(s)} \\ & - \frac{u(1 - v)}{u_j} \mathbf{p}_{UR} - \frac{uv}{u_j} \mathbf{p}_{UL}^{(s)} \end{aligned} \quad (41)$$

where $u_i = (i - 1)/(N_{LE} - 1)$ and where the functions $f_u(u)$ and $f_v(u)$ satisfy

$$\mathbf{q}(f_u(u), f_v(u)) = \mathbf{p}_{LETE}(s_{LE}u). \quad (42)$$

For a given value of u , $f_u(u)$ and $f_v(u)$ can be evaluated using a Newton-Raphson search.

In the above expressions, the trans-finite interpolation is implemented by the function $\mathbf{q}(u, v)$. Notice that because $\mathbf{c}_6(0) = \mathbf{p}_{LL}$ and $\mathbf{c}_7(0) = \mathbf{p}_{LR}^{(s)}$, one gets $\mathbf{q}(0, v) = \mathbf{p}_3(v)$ and therefore $\mathbf{c}_{LE1}(v) = \mathbf{c}_3(v)$. Similarly, $\mathbf{q}(u_j, v) = \mathbf{p}_c(v)$. Also, for any u , $\mathbf{q}(u, 0) = \mathbf{p}_6(u)$ and $\mathbf{q}(u, 1) = \mathbf{p}_7(u)$. On the other hand, it is not true that $\mathbf{c}_{LEi}(\frac{1}{2})$ is equal to the value of \mathbf{x}_1 on blade cut i , a property we wish to enforce so that the location of the leading edge can be obtained easily and so that there is no mismatch in curve spacing as one passes from the blade cuts to the non-planar curves. For that reason

the parameterization is modified as shown by the functional dependence of $\mathbf{p}(u, v)$ on $\mathbf{q}(u, v)$ in Eqs. (38)–(40).

Since $\mathbf{q}\left(0, \frac{1}{2}\right) = \mathbf{p}_3\left(\frac{1}{2}\right) = \mathbf{p}_{LETE}(0)$ (this is the blade parameter for the point where the leading edge meets the hub), it follows that $f_u(0) = 0$ and $f_v(0) = \frac{1}{2}$. Similarly we find that $f_u(u_j) = u_j$ and $f_v(u_j) = \frac{1}{2}$. Therefore it also follows that

$$\xi(0, v) = 0; \quad \xi(u_j, v) = u_j; \quad \xi(u, 0) = \xi(u, 1) = 0; \quad (43)$$

$$\eta(0, v) = \eta(u_j, v) = v; \quad \eta(u, 0) = 0; \quad \eta(u, 1) = 1 \quad (44)$$

and therefore that

$$\mathbf{p}(0, v) = \mathbf{p}_3(v), \quad \mathbf{p}(u_j, v) = \mathbf{p}_c(v), \quad \mathbf{p}(u, 0) = \mathbf{p}_6(u), \quad \mathbf{p}(u, 1) = \mathbf{p}_7(u). \quad (45)$$

Moreover,

$$\xi(u, \frac{1}{2}) = f_u(u); \quad \eta(u, \frac{1}{2}) = f_v(u) \quad (46)$$

so that

$$\mathbf{p}\left(u, \frac{1}{2}\right) = \mathbf{q}\left(f_u(u), f_v(u)\right) = \mathbf{p}_{LETE}(s_{LE}u) \quad (47)$$

as desired. In other words, the change in parameterization from $\mathbf{q}(u, v)$ to $\mathbf{p}(u, v)$ does not affect the edge curves used in the trans-finite interpolation, but it does alter the points at the leading edge so that the curves match the blade cuts there.

The value of j is obtained from a point on the leading edge specified using its parameter in \mathbf{c}_{LETE} , which will be denoted s_j . Blade cut j is the first whose leading edge point \mathbf{x}_1 lies above this point: i.e. j is the smallest integer such that $u_j s_{LE} > s_j$. To ensure that blade cut j is outside the smoothing range, it is necessary that $(s_j - s_{tip})L > d_t$ which can be rewritten as

$$s_j > s_{tip} + \frac{d_t}{L}. \quad (48)$$

If s_j is too close to the tip, the leading edge curves will show significant curvature: for example, see Fig. 8. This is because the blade cuts near the tip are highly curved in blade parameter space. The trans-finite interpolation propagates the curvature of blade cut j to the remaining non-planar leading edge curves. Choosing s_j to be about half-way along the leading edge usually works well.

In a similar fashion, N_{TE} curves around the trailing edge can be determined using the curves \mathbf{c}_1 , \mathbf{c}_5 and \mathbf{c}_8 .

For reasons described in Sec. 9, the number of curves wrapping around the leading edge should equal the number of curves wrapping around the trailing edge. Therefore, N_{LE} and N_{TE} are defined as

$$N_{LE} = N_{TE} = \left\lceil \frac{\max(1 - s_{LE}, s_{TE})L}{\Delta c} \right\rceil + 1 \quad (49)$$

which ensures that the maximum spacing between the curves, measured along the leading or trailing edge, is Δc .

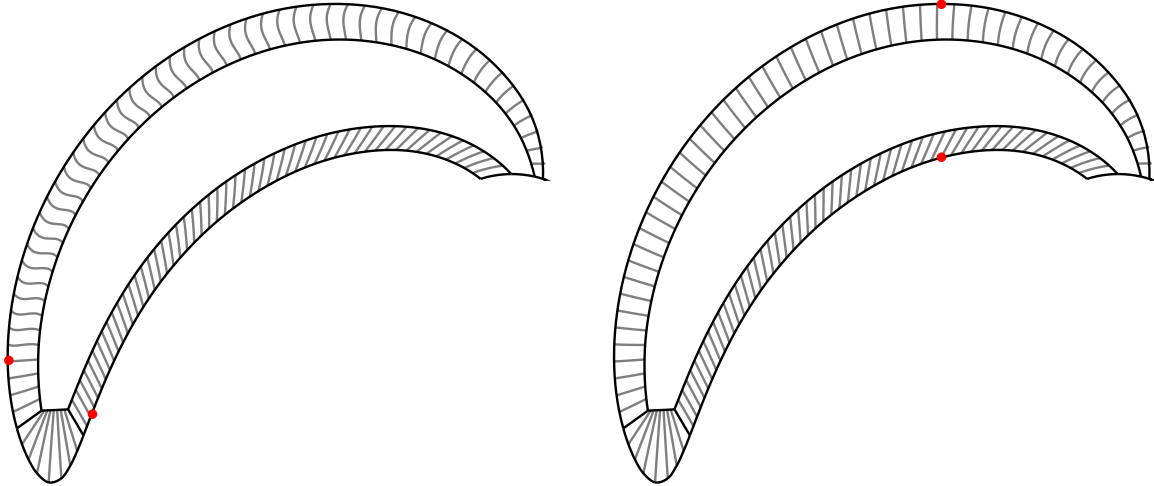


Figure 8: The effect of the location of s_j (shown by the red dots) on the leading and trailing edge curves of a highly skewed blade. When s_j is close to the tip (left) the curves can show excessive curvature; lowering s_j (right) makes a significant improvement.

9 Making spline representations of the surfaces

The following steps are used to create the smoothed blade surfaces by splining the curves around the leading and trailing edges.

1. Using the algorithm described below, find a single knot sequence, ξ_i , that allows each of the curves to be approximated by a spline to within a given accuracy.
2. For the leading edge surface, construct a second knot sequence, η_j , using

$$\eta_j = \frac{j - 1}{N_{LE} - 1}. \quad (50)$$

For each j , sample curve j at ξ_i to obtain the value \mathbf{x}_{ij} . Calculate a two-parameter spline which interpolates the values \mathbf{x}_{ij} at the parameters (ξ_i, η_j) . The spline is the leading edge surface.

The tip and trailing edge surfaces are generated in a similar way.

3. In the blade parameter space, sample the edges of the central surfaces where the end-points of the curves meet the edges.
4. Use trans-finite interpolation to create a grid of sample points in the blade parameter space. Note that this step requires the number of sample points on the left edge to equal the number of sample points on the right edge: i.e. N_{LE} must equal N_{TE} .

5. Spline the sampled points and replace the central surfaces with the splined surfaces.

Because, on their common edges, the same set of points is used for the spline of the central surface and the leading/trailing edge surfaces, these surfaces will match exactly along their common edge. Similarly, the central surfaces will match the upper surface exactly along their common edges.

In Ref. 6, Sec. 11, an algorithm is described for defining a spline approximation to an arbitrary curve by inserting knots into an initial knot sequence until the spline and the curve differ by less than a specified accuracy. For the current purpose, the crucial feature of this algorithm is that it maintains the initial knot sequence as a subset of the final knot sequence. The algorithm can be used to construct the common knot sequence used for each of the curves around the leading and trailing edges:

1. Choose an initial knot sequence, then use the above algorithm to find a spline approximating the first curve to the required accuracy.
2. For each subsequent curve, use the knot sequence from the spline approximation to the previous curve to initialize a spline approximation to the current curve.
3. Obtain the knot sequence from the final curve.

Notice that the knot sequence from the final curve contains the knot sequences used for all the previous curves and therefore, when it is used to reconstruct spline approximations for the curves, each of those approximations will meet the required accuracy.

10 Defining the hub surface

The hub is an axisymmetric surface specified by a curve, the spine, which is rotated about the propeller axis. The hub is split into sectors, one for each blade. The edge of each sector runs roughly parallel to the line on the hub joining the leading and trailing edges of its blade, tracing a helical shape as it extends to the ends of the hub. The intersection of the hub and the reference blade is calculated and the hub sectors are trimmed by removing the footprints of the blades. Only the surfaces on the reference blade and the hub sector associated with the reference blade are saved in the IGES file: Fig. 9 shows a propeller along with the decomposition of the blade and hub surface as saved in the IGES file. The full propeller can be generated by making rotated copies of these surfaces.

The hub surface is parameterized using $\mathbf{p}_h = (\xi, \theta)$ where ξ is between ξ_{lo} at the upstream end and ξ_{hi} at the downstream end. The parameter θ is the angle of rotation around the axisymmetric hub surface. The hub surface is then denoted $\mathbf{h}(\mathbf{p})$.

The DRDC propeller geometry classes provide a curve, $\mathbf{p}_b(u)$, such that $\mathbf{c}_{h0} = \mathbf{h}(\mathbf{p}_b(u))$ lies on the intersection of the blade and hub for all $u \in [0, 1]$. This curve is used for the inner boundary of the trimmed hub sector.

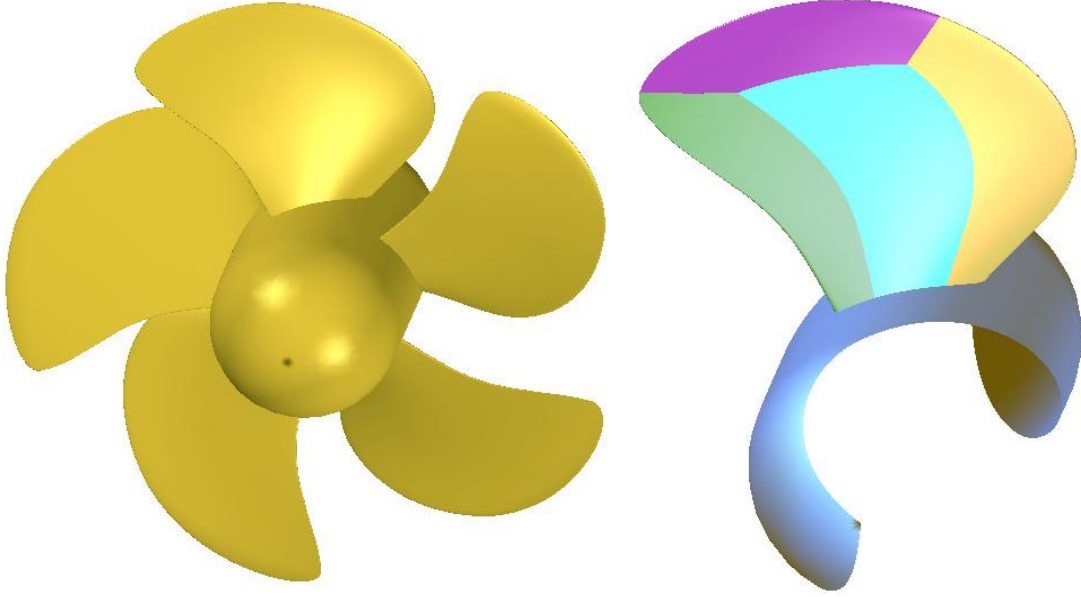


Figure 9: The full propeller (left) and the portion saved in the IGES file (right). Four of the five blade surfaces can be seen. The fifth is in the centre of the other side of the blade.

The outer boundary of the trimmed hub sector is made as follows:

1. Find hub parameters at the leading and trailing edges. Call them (ξ_{le}, θ_{le}) and (ξ_{te}, θ_{te}) .
2. Extrapolate the line joining these two points to the upstream and downstream ends of the hub to obtain two more points, (ξ_{lo}, θ_{lo}) and (ξ_{hi}, θ_{hi}) , where ξ_{lo} and ξ_{hi} are the values of hub parameter ξ at the upstream and downstream ends of the hub. The values of θ_{lo} and θ_{hi} are required to lie in $[-\pi, \pi]$ because the hub surface, when stored in the IGES file, is restricted to this range.

$$\theta_{lo} = \max\left(-\pi, \theta_{le} - \frac{1}{2}m(\xi_{le} - \xi_{lo})\right); \quad (51)$$

$$\theta_{hi} = \min\left(\pi, \theta_{te} + \frac{1}{2}m(\xi_{hi} - \xi_{te})\right); \quad (52)$$

$$m = \frac{\theta_{te} - \theta_{le}}{\xi_{te} - \xi_{le}}. \quad (53)$$

3. Make a Hermite spline (see Ref. 6, Sec. 8) through the four points which is parameterized using ξ . The slope at the two end points is zero and the slope at the leading and trailing edge points is m . This yields a curve, $\mathbf{p}_h(\xi)$, in hub parameter space which passes through the leading and trailing edges and meets the lines $\xi = \xi_{lo}$ and $\xi = \xi_{hi}$ orthogonally.

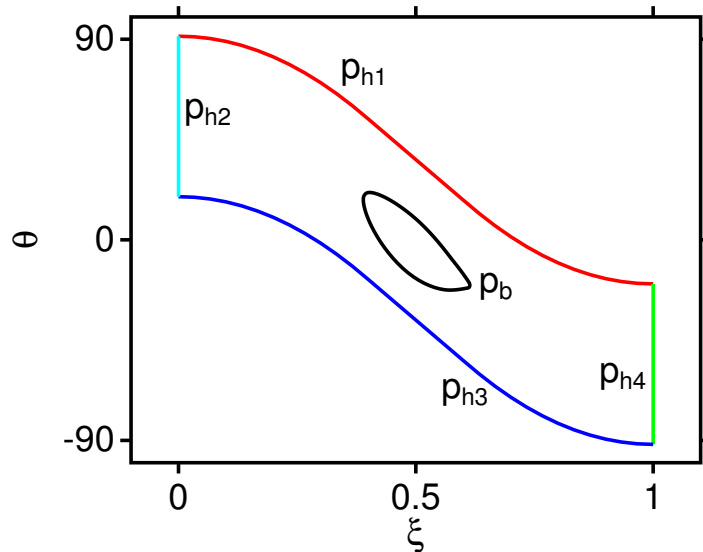


Figure 10: The curves delimiting the hub sector in the hub parameter space.

4. Offset the curve by $\Delta\theta = \pi/Z$, where Z is the number of blades, to obtain a new curve, $\mathbf{p}_{h1}(\xi)$, which passes between the blades.

$$\mathbf{p}_{h1}(u) = \mathbf{p}_h(\xi_{lo} + u(\xi_{hi} - \xi_{lo})) + (0, \pi/Z); \quad (54)$$

$$u = \xi_{lo} + \frac{\xi - \xi_{lo}}{\xi_{hi} - \xi_{lo}}. \quad (55)$$

5. The curve $\mathbf{p}_{h1}(\xi)$ marks one edge of the hub sector in hub parameter space. The opposing edge is made by offsetting $\mathbf{p}_h(\xi)$ by $\Delta\theta = -\pi/Z$ and reversing the parameterization so that it is oriented from the downstream end to the upstream end:

$$\mathbf{p}_{h3}(u) = \mathbf{p}_{h1}(1 - u) - (0, 2\pi/Z). \quad (56)$$

6. The ends of the curves $\mathbf{p}_{h1}(\xi)$ and $\mathbf{p}_{h3}(\xi)$ are joined by two straight lines in hub parameter space:

$$\mathbf{p}_{h2}(u) = (1 - u)\mathbf{p}_{h1}(0) + u\mathbf{p}_{h3}(1); \quad (57)$$

$$\mathbf{p}_{h4}(u) = (1 - u)\mathbf{p}_{h3}(0) + u\mathbf{p}_{h1}(1). \quad (58)$$

7. The union of the four curves $\mathbf{c}_{h1}(u) = \mathbf{h}(\mathbf{p}_{h1}(u))$, $\mathbf{c}_{h2}(u) = \mathbf{h}(\mathbf{p}_{h2}(u))$, $\mathbf{c}_{h3}(u) = \mathbf{h}(\mathbf{p}_{h3}(u))$ and $\mathbf{c}_{h4}(u) = \mathbf{h}(\mathbf{p}_{h4}(u))$ marks the outer edge of the hub sector.

Fig. 10 shows the limiting curves of the hub sector in hub parameter space.

11 Saving the geometry in an IGES file

Once the blade surfaces have been represented as two-parameter splines, they are in a form suitable for saving in an IGES file. This can be done using the classes described in Ref. 7. If the surfaces are C^2 , they will be stored as Rational B-spline Surfaces (entity type 128); otherwise they are stored as Parametric Spline Surface Entities (entity type 114).

The hub is also saved as a surface of revolution trimmed so that only the sector associated with the reference blade is kept (see Sec. 10); the blade footprint is also trimmed away. The trimmed hub is stored as Trimmed (Parametric) Surface Entity (entity type 144) which contains a Surface of Revolution Entity (entity type 120) with an outer bounding curve to define the limit of the hub sector, and an inner bounding curve to define the blade footprint.

The Surface of Revolution Entity which defines the untrimmed hub contains a curve, the spine, which is rotated about the z axis to generate the surface. The DRDC propeller geometry classes provide a representation of the spine, but not in a form directly compatible with the IGES format. It is first converted to a spline and saved as a Rational B-spline Curve Entity (entity type 126) if the spine is C^2 , or a Parametric Spline Curve Entity (entity type 112) if it is not. The spline is determined so that the accuracy of the approximation is consistent with the accuracy used when calculating the blade surfaces.

The inner boundary of the trimmed hub sector is the blade-hub intersection curve, \mathbf{c}_{h0} . The DRDC description of the propeller provides a representation of this curve, but not in a form understood by the IGES format. The curve is approximated by a spline in the hub parameter space, to a similar accuracy as used by the blade splines, which is used to define a Curve on a Parametric Surface Entity (entity type 142).

The outer boundary of the hub sector is also a Curve on a Parametric Surface Entity with the curve in the hub parameter space defined by a Composite Curve Entity (entity type 102) used to concatenate the four edges of the hub sector, \mathbf{c}_{h1} , \mathbf{c}_{h2} , \mathbf{c}_{h3} and \mathbf{c}_{h4} , into a single curve. The degenerate curves at the ends of the hub are each represented as a Line Entity (entity type 110) while the two curves delineating the edges of the hub sector are Parametric Spline Curve Entities.

12 Concluding remarks

The algorithms describe in this report circumvent a common problem when a propeller is generated in the traditional way from a series of airfoil sections: a coordinate singularity causes the geometry to be poorly defined near the tip so that it is not suitable for use in Reynolds-averaged Navier-Stokes (RANS) flow solvers. The algorithms remove the coordinate singularity and smooth the tip in a controlled way.

The smoothed geometry is written in the IGES format which can be used by most commercial flow solvers. The improvements in propeller geometry allow analyses of propellers to be performed with a minimum of effort. The analysis procedure will be more robust and the results more reliable.

References

- [1] Hally, D. (2013), C++ classes for representing propeller geometry, (DRDC Atlantic TM 2013-177) Defence Research and Development Canada – Atlantic.
- [2] Hally, D. (2013), User’s guide for smooth-prop: a program to smooth propeller tip geometry, (DRDC Atlantic TM 2013-179) Defence Research and Development Canada – Atlantic.
- [3] (1988), Initial Graphics Exchange Specification (IGES) Version 4.0, US Dept. of Commerce, National Bureau of Standards. Document No. NBSIR 88-3813.
- [4] Hally, D. (2013), A procedure to create CFD meshes around propellers, (DRDC Atlantic TM 2013-180) Defence Research and Development Canada – Atlantic.
- [5] Hally, D. (2006), C++ classes for representing curves and surfaces: Part IV: Distribution functions, (DRDC Atlantic TM 2006-257) Defence Research and Development Canada – Atlantic.
- [6] Hally, D. (2006), C++ classes for representing curves and surfaces: Part II: Splines, (DRDC Atlantic TM 2006-255) Defence Research and Development Canada – Atlantic.
- [7] Hally, D. (2006), C++ classes for representing curves and surfaces: Part III: Reading and writing in IGES format, (DRDC Atlantic TM 2006-256) Defence Research and Development Canada – Atlantic.

List of symbols

α	The smoothing relaxation factor.
β_i	Relaxation factors for the Laplace filter.
$\eta_h(\xi)$	A function of blade parameter ξ such that $\mathbf{b}(\xi, \eta_h(\xi))$ lies on the hub. It is sufficient to define the blade/hub intersection in the blade parameter space.
η_{LE}	The blade parameter η for the point \mathbf{x}_{LE} on the leading edge.
η_{TE}	The blade parameter η for the point \mathbf{x}_{TE} on the trailing edge.
θ_{lo}	Hub parameter of the point at the upstream end of the hub extrapolated from the line through the leading and trailing edges.
θ_{hi}	Hub parameter of the point at the downstream end of the hub extrapolated from the line through the leading and trailing edges.
(ξ, η)	Parameters for the blade surface.
(ξ_h, θ)	Parameters for the hub surface.
ξ_{hi}	The value of ξ_h at the downstream end of the hub.
(ξ_{le}, θ_{le})	Hub parameters where the leading edge meets the hub.
ξ_{lo}	The value of ξ_h at the upstream end of the hub.
ξ_{LL}	The blade ξ parameter of the lower left corner of the central surface.
ξ_{LR}	The blade ξ parameter of the lower right corner of the central surface.
(ξ_{te}, θ_{te})	Hub parameters where the trailing edge meets the hub.
(ξ_{UL}, η_{UL})	The blade parameters for the upper left corner of the central blade surface.
(ξ_{UR}, η_{UR})	The blade parameters for the upper right corner of the central blade surface.
$a_i(u)$	Arclength distributions.
$\mathbf{c}_i(u)$	Curves used as edges for the five blade surfaces: $i \in [1, 12]$.
$\mathbf{b}(\mathbf{p})$	A function returning points on the surface of the reference blade.
$\mathbf{c}_{hi}(u)$	Curves used as edges for the hub surface: $i \in [1, 4]$.

$\mathbf{c}_i(u)$	Curves used as edges for the five blade surfaces: $i \in [1, 12]$.
$\mathbf{c}_{LETE}(s)$	A curve along the leading and trailing edges parameterized using fractional arclength.
$\mathbf{h}(\mathbf{p}_h)$	A function returning points on the surface of the hub.
d	The maximum separation of the points used for smoothing a blade cut.
d_e	On a blade cut, the distance from the leading or trailing edge over which smoothing occurs.
d_{LR}	The distance of \mathbf{x}_{LR} from the leading edge at the hub.
d_{UR}	The distance of \mathbf{x}_{UR} from \mathbf{x}_{LE} .
d_t	The distance from the tip, measured as arclength along the leading and trailing edge, over which smoothing occurs.
$f(x)$	Function used to modulate the amount of smoothing of a blade cut. Also used for the distribution function governing the points sampled on a blade cut.
h	The minimum separation of the points used for smoothing a blade cut.
L	Arclength around the blade outline.
N_{LE}	the number of curves around the leading edge.
N_{TE}	the number of curves around the trailing edge.
\mathbf{n}	A normal to a surface.
\mathbf{p}	A two-vector giving parameters for a point on the blade: equivalent to (ξ, η) .
$\mathbf{p}_b(u)$	A curve in hub parameter space for the blade-hub intersection.
\mathbf{p}_h	A two-vector giving parameters for a point on the hub: equivalent to (ξ_h, θ) .
$\mathbf{p}_{hi}(u)$	Curves in hub parameter space corresponding to $\mathbf{c}_{hi}(u)$: i.e. $\mathbf{h}(\mathbf{p}_{hi}(u)) = \mathbf{c}_{hi}(u)$.
$\mathbf{p}_i(u)$	Curves in blade parameter space corresponding to $\mathbf{c}_i(u)$: i.e. $\mathbf{b}(\mathbf{p}_i(u)) = \mathbf{c}_i(u)$.
$\mathbf{p}_{LETE}(s)$	Curves in blade parameter space corresponding to $\mathbf{c}_{LETE}(s)$.

\mathbf{p}_{LL}	The blade parameter for the point on the blade-hub intersection at the lower left hand corner of the central surface on the pressure side of the blade.
\mathbf{p}_{LR}	The blade parameter for the point on the blade-hub intersection at the lower right hand corner of the central surface on the pressure side of the blade.
\mathbf{p}_{UL}	The blade parameter for the point at the upper left hand corner of the central surface on the pressure side of the blade.
\mathbf{p}_{UR}	The blade parameter for the point on the blade hub intersection at the upper right hand corner of the central surface on the pressure side of the blade.
\mathbf{p}_{LE}	The blade parameter for the point on the leading edge between the leading edge surface and the tip surface.
\mathbf{p}_{TE}	The blade parameter for the point on the trailing edge between the trailing edge surface and the tip surface.
$\mathbf{q}(u, v)$	Trans-finite interpolation function used to define the parameter curves for the leading and trailing edge curves outside the smoothing limits.
s	The parameter of the curve \mathbf{c}_{LETE} : the fractional arclength along the curve along the leading and trailing edges.
s_{LE}	The value of s for which $\mathbf{c}_{LETE}(s_{LE}) = \mathbf{x}_{LE}$.
s_{TE}	The value of s for which $\mathbf{c}_{LETE}(s_{TE}) = \mathbf{x}_{TE}$.
s_{tip}	The value of s for which $\mathbf{c}_{LETE}(s_{tip})$ is the blade tip.
\mathbf{t}	A tangent to a blade cut.
\mathbf{x}_{LL}	The point on the blade-hub intersection at the lower left hand corner of the central surface on the pressure side of the blade.
\mathbf{x}_{LR}	The point on the blade-hub intersection at the lower right hand corner of the central surface on the pressure side of the blade.
\mathbf{x}_{UL}	The point at the upper left hand corner of the central surface on the pressure side of the blade.
\mathbf{x}_{UR}	The point on the blade hub intersection at the upper right hand corner of the central surface on the pressure side of the blade.

\mathbf{x}_{LE}	The point on the leading edge between the leading edge surface and the tip surface.
\mathbf{x}_{TE}	The point on the trailing edge between the trailing edge surface and the tip surface.
\mathbf{y}_i^n	Points on a blade cut after n smoothing iterations.
Z	The number of propeller blades.

DOCUMENT CONTROL DATA		
(Security markings for the title, abstract and indexing annotation must be entered when the document is Classified or Designated.)		
1. ORIGINATOR (The name and address of the organization preparing the document. Organizations for whom the document was prepared, e.g. Centre sponsoring a contractor's report, or tasking agency, are entered in section 8.) Defence Research and Development Canada – Atlantic PO Box 1012, Dartmouth NS B2Y 3Z7, Canada	2a. SECURITY MARKING (Overall security marking of the document, including supplemental markings if applicable.) UNCLASSIFIED	2b. CONTROLLED GOODS (NON-CONTROLLED GOODS) DMC A REVIEW: GCEC APRIL 2011
3. TITLE (The complete document title as indicated on the title page. Its classification should be indicated by the appropriate abbreviation (S, C or U) in parentheses after the title.) Smoothing propeller tip geometry for use in a RANS solver		
4. AUTHORS (Last name, followed by initials – ranks, titles, etc. not to be used.) Hally, D.		
5. DATE OF PUBLICATION (Month and year of publication of document.) October 2013	6a. NO. OF PAGES (Total containing information. Include Annexes, Appendices, etc.) 38	6b. NO. OF REFS (Total cited in document.) 7
7. DESCRIPTIVE NOTES (The category of the document, e.g. technical report, technical note or memorandum. If appropriate, enter the type of report, e.g. interim, progress, summary, annual or final. Give the inclusive dates when a specific reporting period is covered.) Technical Memorandum		
8. SPONSORING ACTIVITY (The name of the department project office or laboratory sponsoring the research and development – include address.) Defence Research and Development Canada – Atlantic PO Box 1012, Dartmouth NS B2Y 3Z7, Canada		
9a. PROJECT OR GRANT NO. (If appropriate, the applicable research and development project or grant number under which the document was written. Please specify whether project or grant.) Project 01gl08	9b. CONTRACT NO. (If appropriate, the applicable number under which the document was written.)	
10a. ORIGINATOR'S DOCUMENT NUMBER (The official document number by which the document is identified by the originating activity. This number must be unique to this document.) DRDC Atlantic TM 2013-178	10b. OTHER DOCUMENT NO(s). (Any other numbers which may be assigned this document either by the originator or by the sponsor.)	
11. DOCUMENT AVAILABILITY (Any limitations on further dissemination of the document, other than those imposed by security classification.) <input checked="" type="checkbox"/> Unlimited distribution <input type="checkbox"/> Defence departments and defence contractors; further distribution only as approved <input type="checkbox"/> Defence departments and Canadian defence contractors; further distribution only as approved <input type="checkbox"/> Government departments and agencies; further distribution only as approved <input type="checkbox"/> Defence departments; further distribution only as approved <input type="checkbox"/> Other (please specify):		
12. DOCUMENT ANNOUNCEMENT (Any limitation to the bibliographic announcement of this document. This will normally correspond to the Document Availability (11). However, where further distribution (beyond the audience specified in (11)) is possible, a wider announcement audience may be selected.)		

13. ABSTRACT (A brief and factual summary of the document. It may also appear elsewhere in the body of the document itself. It is highly desirable that the abstract of classified documents be unclassified. Each paragraph of the abstract shall begin with an indication of the security classification of the information in the paragraph (unless the document itself is unclassified) represented as (S), (C), or (U). It is not necessary to include here abstracts in both official languages unless the text is bilingual.)

The traditional method of specifying propeller geometry is to define a series of airfoil sections each of which is modified by local values of the chord length, pitch, skew angle and rake. Near the tip of the propeller, where the chord length reduces rapidly to zero, a blade defined in this way often has surface irregularities which make meshing for flow solvers difficult. Methods are described for smoothing the irregularities and saving the resulting propeller geometry in the IGES format which can be read by most flow solvers.

14. KEYWORDS, DESCRIPTORS or IDENTIFIERS (Technically meaningful terms or short phrases that characterize a document and could be helpful in cataloguing the document. They should be selected so that no security classification is required. Identifiers, such as equipment model designation, trade name, military project code name, geographic location may also be included. If possible keywords should be selected from a published thesaurus. e.g. Thesaurus of Engineering and Scientific Terms (TEST) and that thesaurus identified. If it is not possible to select indexing terms which are Unclassified, the classification of each should be indicated as with the title.)

Propellers
Computational fluid dynamics
Fluid flow
IGES
ANSYS CFX

This page intentionally left blank.

Defence R&D Canada

Canada's leader in defence
and National Security
Science and Technology

R & D pour la défense Canada

Chef de file au Canada en matière
de science et de technologie pour
la défense et la sécurité nationale



www.drdc-rddc.gc.ca